Feasibility study of friction stir welding of 6061-T6 aluminium alloy with AISI 1018 steel

W H Jiang and **R Kovacevic***
Research Centre for Advanced Manufacturing, Southern Methodist University, Richardson, Texas, USA

Abstract: The present work demonstrates that friction stir welding (FSW) is a feasible route for joining 6061 aluminium (Al) alloy to AISI 1018 steel. The weld has a good weld quality and is free of cracks and porosity. The tensile failure happened at the boundary between the nugget and thermomechanically affected zone of the base Al alloy, indicating that the weld has a higher joining strength. Despite the fact that the hardness fluctuates strongly within the nugget, the average hardness of the nugget is substantially higher than that of the base Al alloy. During FSW, localized melting of the Al alloy in the nugget occurred, and the molten Al alloy reacted strongly with steel pieces spread through the nugget, which resulted in the formation of the Al–Fe intermetallic compounds, $Al_{13}Fe_4$ and Al_5Fe_2. The nugget consists of secondary phases including coarse steel pieces and Al–Fe intermetallic compounds, and an Al alloy matrix. These secondary phases contribute to the hardness of the weld.

Keywords: friction stir welding, steel, Al alloy, intermetallic compounds

1 INTRODUCTION

Aluminium (Al) alloys and steels form an interesting combination from the viewpoint of application, especially in the automotive industry. However, the joining of such materials is a challenge, and conventional fusion welding does not provide a good weld owing to significant differences in physical properties such as melting points and thermal expansion coefficients, which tend to introduce various welding defects such as solidification cracks, liquation cracks and porosity. In order to obtain faultlessly welded joints, specially chosen filler materials that have a good metallurgical compatibility with both base materials are indispensable. However, the filler materials are usually noble metals and, thus, expensive. Some efforts have been made to use various solid-state bonding techniques, mainly friction welding [**1**–**4**] and ultrasonic welding [**5**]. However, despite the good bonding that can be achieved, there are strict limitations to the geometry of components that could be welded with these techniques. For example, the friction weld is applied only to cylinders such as pipes and rods, while the ultrasonic weld is limited to foils or very thin sheets.

The MS was received on 21 October 2003 and was accepted after revision for publication on 14 June 2004.
**Corresponding author: Research Centre for Advanced Manufacturing, School of Engineering, Southern Methodist University, 1500 International Parkway, Suite 100, Richardson, TX 75081, USA. E-mail: kovacevic@engr.smu.edu*

As a novel joining process, friction stir welding (FSW) has emerged as a promising solid-state welding process. It has demonstrated several advantages over the fusion welding process due to the solid-state nature of the process, such as the elimination of various solidification defects. In the past decade, FSW has revolutionized the welding of Al alloys and achieved a high level of maturity for the joining of such materials. A wide variety of both the same and dissimilar Al alloys has been successfully processed using this technique. While most of the FSW efforts to date have involved the joining of Al alloys, there is considerable interest in extending the technology to other metallic materials including steels. It has been demonstrated that it is feasible for FSW to join mild steels [**6**] and stainless steels [**7**].

Watanabe *et al*. [**8**] reported the joining of steel to an aluminium alloy 2 mm thick by interface-activated adhesion welding with a preliminary satisfactory joint. Recently, Chen and Kovacevic [**9**] reported new findings on successful joining of an aluminium alloy to mild steel by combined effects of fusion and solid state welding.

Although substantial development on FSW has been achieved in the last decade, little work has been performed in the joining of dissimilar materials with a significant difference in physical properties. The present work deals with the application of FSW for joining an Al alloy to a mild steel. The microstructures and hardness distribution of welds are investigated. It is expected that this preliminary work can disclose the applicability of FSW for joining an Al alloy to steel.

Table 1 Nominal chemical composition of 6061 Al alloy and 1018 steel (wt %)

6061 Al alloy	Cu 0.25	Mg 1.0	Mn 0.6	Si 0.6	Al balance
1018 steel	C 0.18	Mn 0.75	P < 0.04	S < 0.05	Fe balance

2 EXPERIMENTAL

With a thickness of 6 mm, a rolled sheet of 6061-T6 Al alloy and a cold-rolled sheet of AISI 1018 mild steel were used in FSW. Their nominal chemical compositions are shown in Table 1. Single-pass friction stir butt welds were made using an FSW tool with a shoulder and pin, 25 mm and 5.5 mm in diameter respectively. The FSW tool was made of an H13 tool steel. The welding direction was longitudinal to the rolled sheets. During the welding process, the sheets were clamped firmly to a backing plate. The rotational speed of the tool was 914 r/min and its traverse speed was 140 mm/min. The rotating pin was inserted into the weld line of the base sheets asymmetrically with about three-quarters of it in the Al alloy side and the remaining one-quarter in the steel side.

During FSW, the temperature of the base alloys near the nugget was measured using K-type thermocouples. The thermocouples were placed at the centre thickness of the sheets about 5 and 2 mm from the original interface between the two sheets in the Al alloy side and the steel side respectively.

A uniaxial tensile test was performed on the weld. A rectangle sample was extracted with the longitudinal direction perpendicular to the welding interface. Microhardness measurements were made along the cross-section of the weld. The load was set at 50 g. Samples were prepared by grinding, polishing and etching. Metallographic specimens were extracted from the S–T (short transverse) plane of the base sheet alloy. Specimens were etched with either Keller's reagent (150 mL H_2O, 3 mL HNO_3, 6 mL HCl, 6 mL HF) or an alcohol solution of 5% HNO_3, which are well-known etchants for Al alloys and steels respectively. An optical microscope and a scanning electron microscope (SEM) were used to observe microstructures. An energy dispersive analysis of X-ray (EDAX) attached to an SEM was used for compositional microanalysis. An X-ray diffraction analysis with Cu $K\alpha$ was performed to identify the phases in the welds. The operating voltage was 40 kV. Only the nuggets were exposed to X-ray radiation and the remaining base materials were covered with pieces of graphite so that the constituents of the nuggets could be identified exactly.

3 RESULTS

A cross-section of the typical welded Al alloy–steel sheet is shown in Fig. 1. No cracks and porosity are visible, indicating a good quality. The weld zone is clearly visible

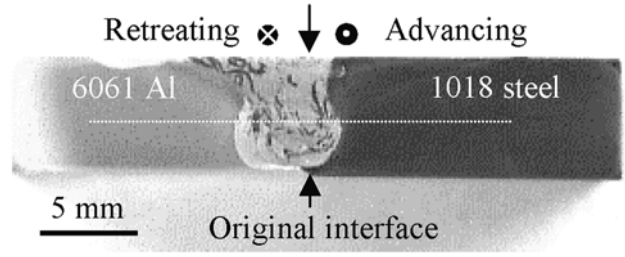

Fig. 1 Overview photograph of the cross-section of the welded sheet material. The line indicates positions where microhardness was measured

because of its different contrasts developed after etching. A weld nugget in the shape of an onion was developed. It is noted that the nugget is asymmetrical with respect to the original interface between the Al alloy and the steel, but about three-quarters of the nugget is within the Al alloy, whereas one-quarter is within the steel. This feature of the weld resulted from the arrangement of the rotating pin with respect to the joint line. Considering the fact that steel has a higher deformation resistance at the weld temperature than the Al alloy, the arrangement of the rotating pin would reduce its wear and prolong its life substantially.

The temperature profiles during FSW in the two base alloys at the centre thickness of the sheets at a distance of 5 and 2 mm from the original interface in the Al alloy and steel respectively are shown in Fig. 2. Evidently, the temperature is not symmetrical with the base alloys. This lack of symmetry may be related to the location of the rotating pin and, particularly, a significant difference in mechanical and physical properties between the Al alloy and steel. The maximum temperatures in the Al alloy and steel are as high as 491 and 613 °C respectively. Undoubtedly, a higher temperature must have been reached within the nugget.

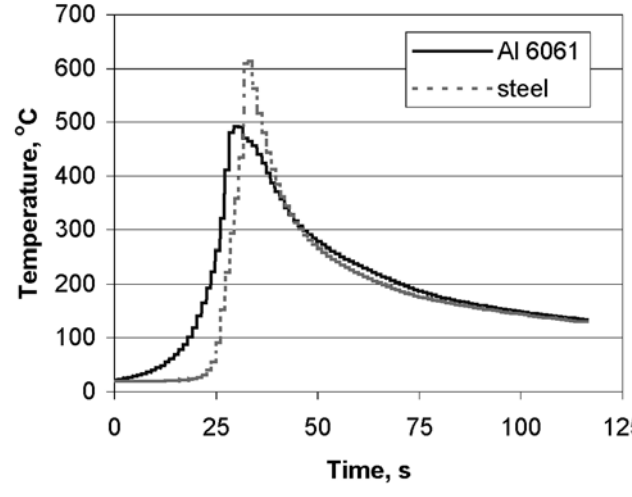

Fig. 2 Temperature profiles at the centre thickness of the sheets at a distance of 5 and 2 mm from the original interface in the Al alloy and steel respectively

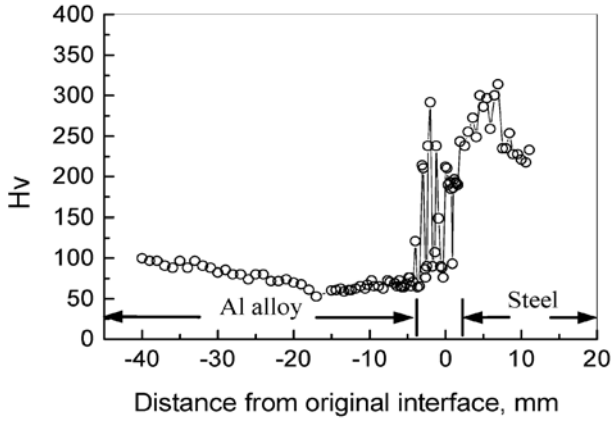

Fig. 3 Microhardness distribution across the nugget

Microhardness was measured along the line indicated in Fig. 1, which represents the cross-section of the nugget. The results are shown in Fig. 3. It can be seen that the hardness distribution is not uniform within the nugget. In some locations it is very high, even higher than that of the base steel, while in other locations it is lower, similar to that of the base Al alloy. However, it can be estimated that the average bulk hardness of the nugget is higher than that of the base Al alloy. As such, the substantial fluctuation must be related to the heterogeneous constitution of the nugget. Furthermore, it can be noted that the zone of the base steel bounded by the nugget, i.e. the thermo-mechanically affected zone (TMAZ), has a higher hardness than the base steel, while the TMAZ in the base Al alloy has a lower hardness than the base Al alloy. This change in hardness must be related to the microstructural evolution during processing.

The tensile test demonstrates that fracture occurred at the boundary between the nugget and the TMAZ in the base Al alloy rather than along the weld interface, as shown in Fig. 4. This indicates that the nugget has a higher joining strength. The ultimate tensile strength of the weld is 117 MPa. For the purpose of comparison, a tensile test was also performed on the base Al alloy with the same geometry as the welded sample and its ultimate tensile strength is 303 MPa.

An X-ray diffraction analysis was performed on the nugget. The resulting diffraction pattern is shown in Fig. 5. The diffraction peaks of carbon are a result of

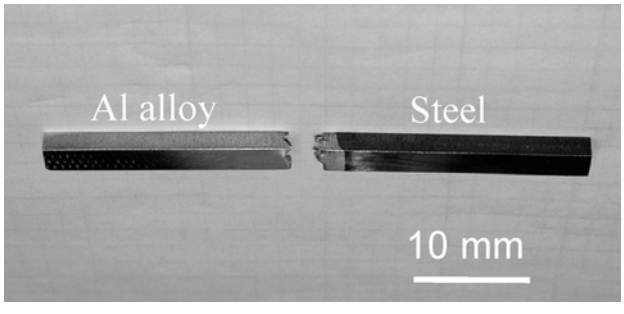

Fig. 4 Photograph of the tensile fractured sample

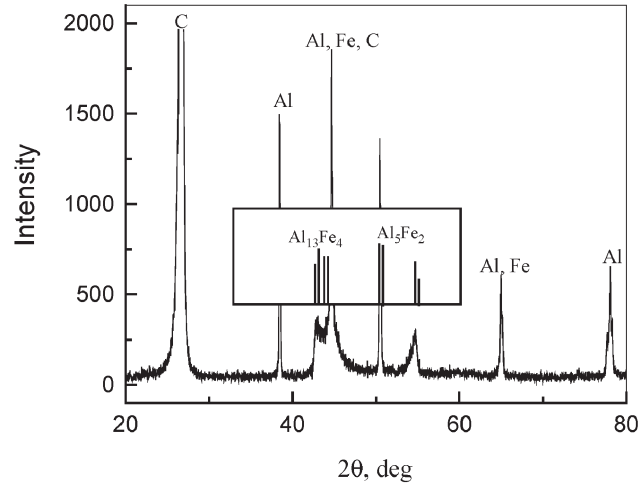

Fig. 5 X-ray diffraction pattern of the nugget. Inset shows the positions of main diffraction peaks of $Al_{13}Fe_4$ and Al_5Fe_2

the covering graphite and the other peaks from the constituent phases in the nugget. It can be seen that besides α-Al and α-Fe, there are $Al_{13}Fe_4$ and Al_5Fe_2 phases in the nugget. This result indicates that during FSW, the Al–Fe intermetallic compounds were formed.

Figure 6 is a magnified overview of the nugget. It can be seen that many relatively coarse, dark pieces in the form of a short ribbon are spread through the nugget. EDAX demonstrates that these sheared-off pieces are mild steel. The steel pieces are well distributed within the nugget except in the lower portion of it near the base Al alloy. Besides the steel pieces, a number of grey blocky particles are visible, whose size is varied. Although they are omnipresent within the nugget, it seems that they are larger in size as well as larger in number in the lower portion of the nugget near the base Al alloy where the steel pieces are deficient. It is known that FSW nuggets of dissimilar alloys such as 6061 Al alloy welded to 2024 Al alloy and 6061 Al alloy welded to copper are characterized by complex vortex-like and swirl-like intercalation [**10**–**12**]. Such characteristic features do not seem to be obvious in the FSW nugget of 6061 Al alloy and 1018 mild steel, despite the fact that the flow pattern is visible in the lower portion of the nugget near the base Al alloy.

Extensive metallographical observations indicate that a strong reaction between the steel pieces and the Al matrix within the nugget occurred, resulting in the formation of Al–Fe intermetallic compounds. Figure 7 shows a typical situation of the reaction at the surface of the steel pieces and precipitates in the matrix of the Al alloy. It can be seen that the precipitates assumed various morphologies, i.e. sphere-like, needle, flower petal and blocky shapes. Their size is varied. Those near the Al alloy side are generally sphere-like and smaller, while those close to the steel side are in the form of a needle and a flower petal, and they are larger.

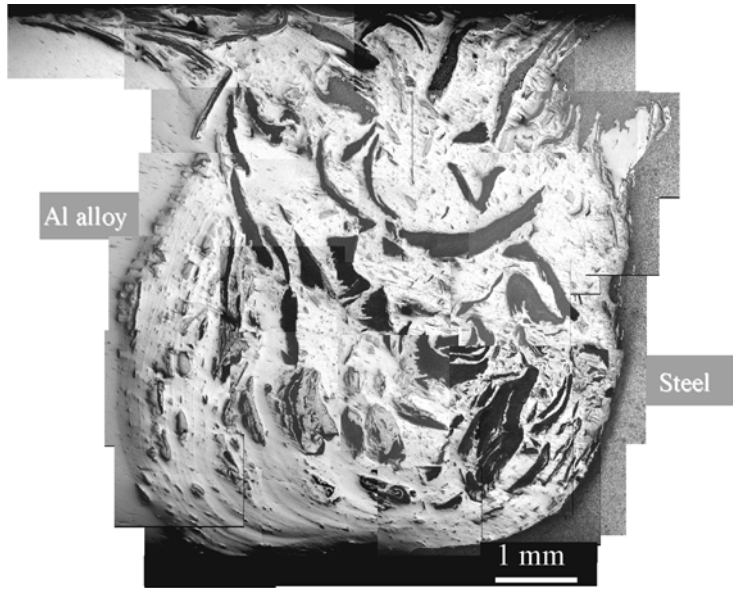

Fig. 6 A magnified view of the nugget

Although the reaction usually occurred at the surface of steel pieces, the reaction within the interior of the steel pieces is also visible, and a typical observation is shown in Fig. 8. In the back-scattered electron image (BEI), the steel pieces appear brightest, the Al alloy matrix darkest and the reaction products grey. Some blocky particles with a layered structure and the segregated clusters of fine precipitates are observable near the Al alloy side (Fig. 9). EDAX demonstrates that each layer within a layered particle has a different composition, as shown in Fig. 10. They are different Al–Fe intermetallic compounds. The darker it appears, the higher the content of Al, and vice versa. Combined with the X-ray diffraction analysis results, it can be deduced that the darker Al-rich layer may be $Al_{13}Fe_4$ and the grey layer Al_5Fe_2. The segregated cluster of fine precipitates, as shown in Fig. 9b, seems to result from the evolution of a blocky particle with the layered structure. The fine precipitates appear darker in a BEI, indicating that they may probably be $Al_{13}Fe_4$. This

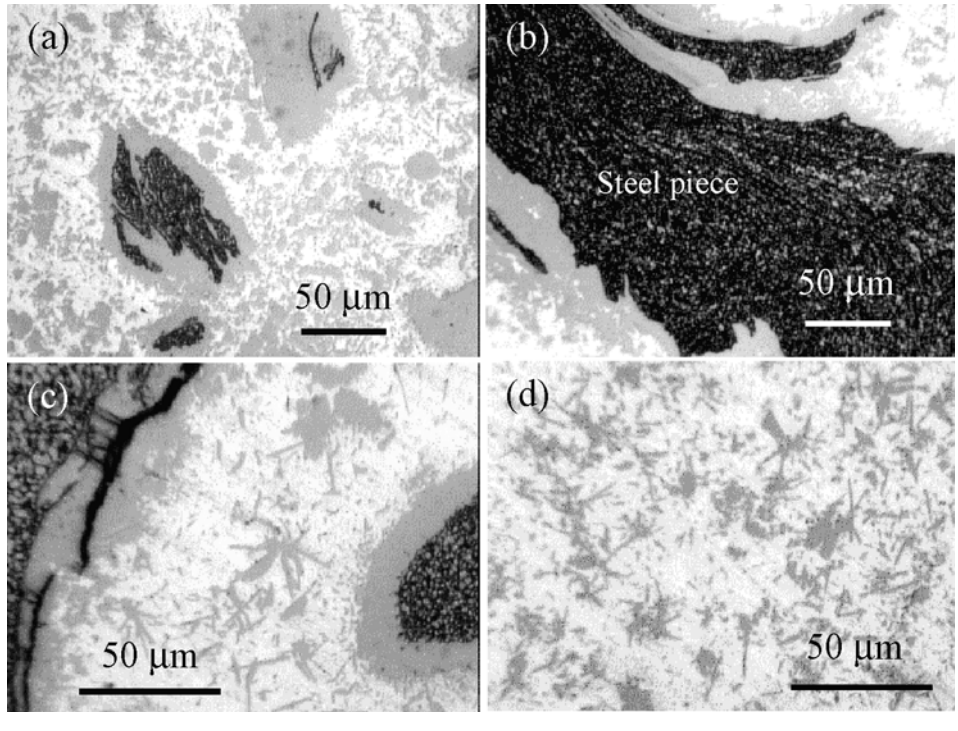

Fig. 7 Micrographs showing a strong reaction between steel pieces and an Al alloy matrix in the nugget

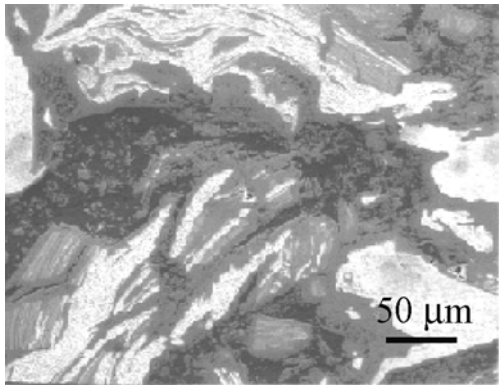

Fig. 8 Back-scattered electron image (BEI) showing the reaction in the interior of steel pieces

result demonstrates that the Al-rich $Al_{13}Fe_4$ seems to be more stable, as it is only one phase in the segregated cluster. The reaction within the interior of steel pieces may be related to an intercalated lamellar structure developed during FSW. Undoubtedly, the reaction between the Al alloy and steel pieces tends to destroy the morphology of intercalation. This may be why few intercalation structures are observable. The severity of the reaction is related to locations. Near the Al alloy side (Fig. 9), the reaction proceeded completely and steel pieces were almost exhausted, while close to the steel side a few of the steel pieces surrounded by the reaction layer remained observable (Fig. 7).

Figure 11 shows the microstructures of steel pieces and an Al alloy matrix in the nugget. Evidently, the steel

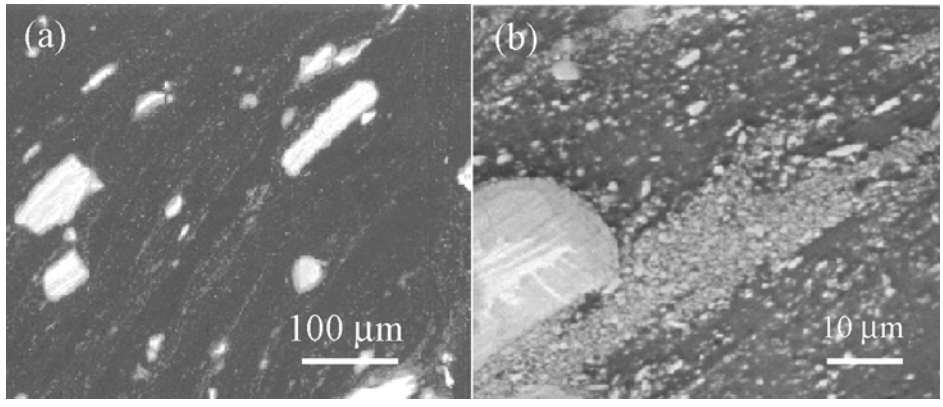

Fig. 9 BEI of the precipitates near the Al alloy side

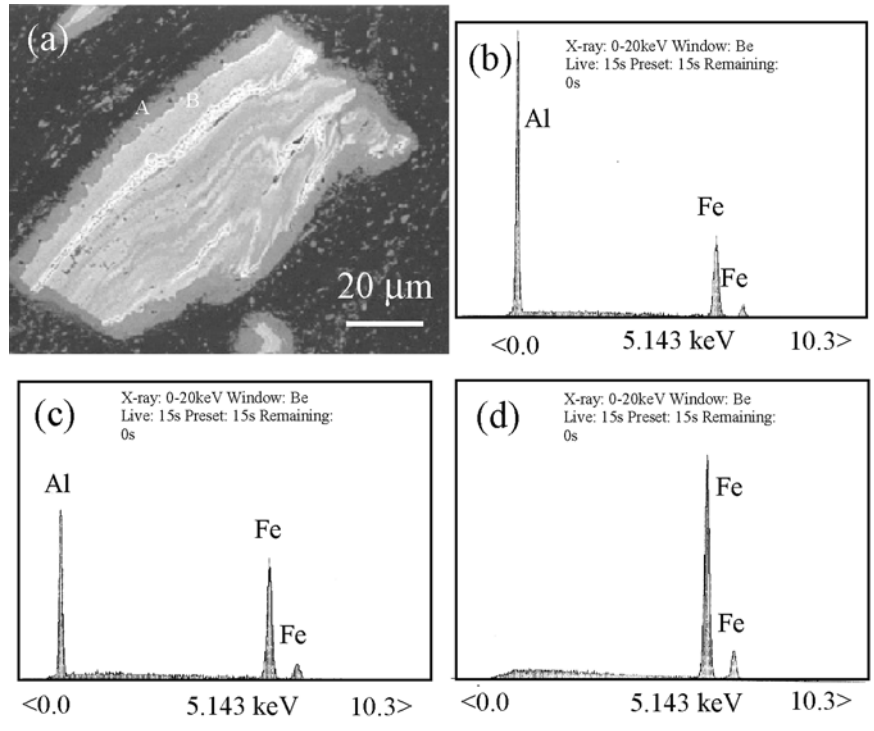

Fig. 10 BEI of a blocky particle with (a) a layered structure and the EDAX spectrum at positions (b) A, (c) B and (d) C

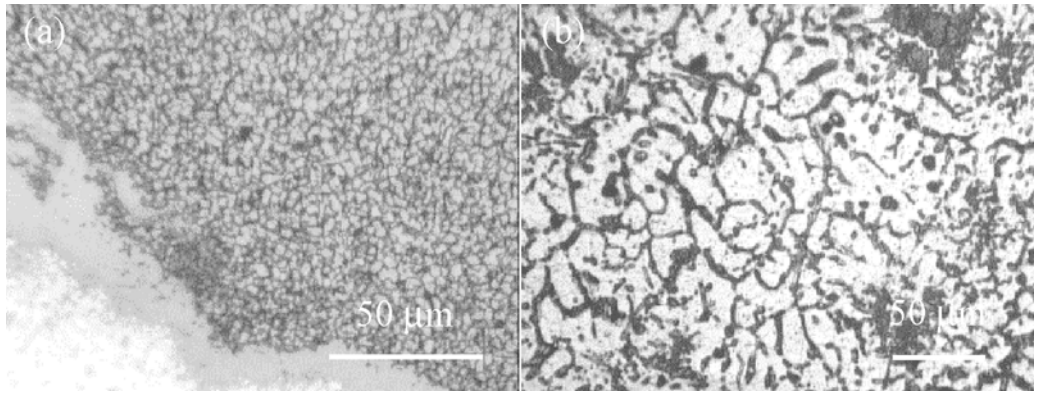

Fig. 11 Microstructures of (a) the steel pieces and (b) an Al alloy matrix in the nugget

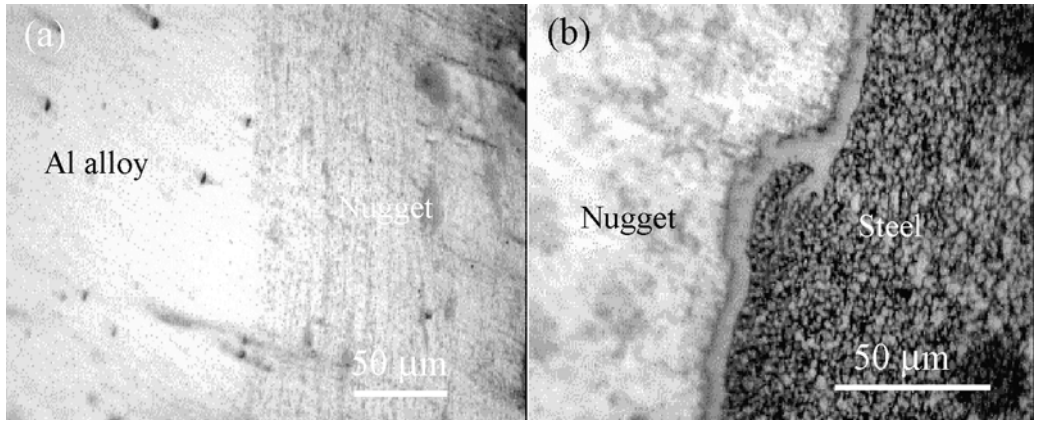

Fig. 12 Microstructures of boundary zones between the nugget and (a) the base Al alloy and (b) steel

pieces have very fine grains, much smaller than those of the base steel that may result from dynamic recrystallization induced by strong friction stirring. The Al alloy matrix also has a fine grain structure, and numerous precipitates are located at the grain boundary.

Figure 12 shows the boundary zones between the base alloys and the nugget. It can be seen that like the steel pieces within the nugget, a reaction layer formed between the base steel and the nugget, while no reaction is visible between the Al alloy and the nugget. Obvious flowing lines of the materials within the nugget near the Al alloy can be seen in Fig. 9a, and fine precipitates are distributed within the material flow lines.

Figure 13 contrasts the microstructures of the TMAZs with those of the base alloys. It can be seen that grains of the TMAZ in the steel are remarkably smaller than those of the base steel, while in the Al alloy they are comparable to those of the base alloy.

4 DISCUSSION

The present work demonstrates that FSW of dissimilar alloys, 6061 Al alloy and AISI 1018 steel, is feasible, and the weld has a good quality and is free of cracks and porosity. The weld has a high joining strength, which is evidenced by the fact that the tensile fracture occurred at the boundary between the nugget and the TMAZ in the base Al alloy rather than along the welding interface. There may be two reasons for this result. Firstly, the TMAZ in the base Al alloy has a lower hardness, as evidenced in Fig. 3. In contrast, it is known that a heat-affected zone (HAZ) of friction stir welded 6000-T6 Al alloy is the weakest location [**13**, **14**]. A loss in strength of an HAZ is definitely related to microstructural evolution such as dissolution and over-ageing of fine precipitates that form during T6 ageing. It is believed that this process also occurs in the case of FSW of the Al alloy with steel. Secondly, the boundary between the nugget and the TMAZ in the base Al alloy may accumulate impurities from the original joint surfaces.

It is worthy of mention that severe wear of FSW tools happened in the present work. A more durable tool material is being identified. The focus of this paper is the microstructural characterization of the nuggets produced in FSW.

The previous work indicated that the welds of dissimilar materials of 6061 Al–Cu are not of good quality, as they had considerable discontinuity and tunnel development [**10**–**12**]. A nugget is subjected to the largest strain and

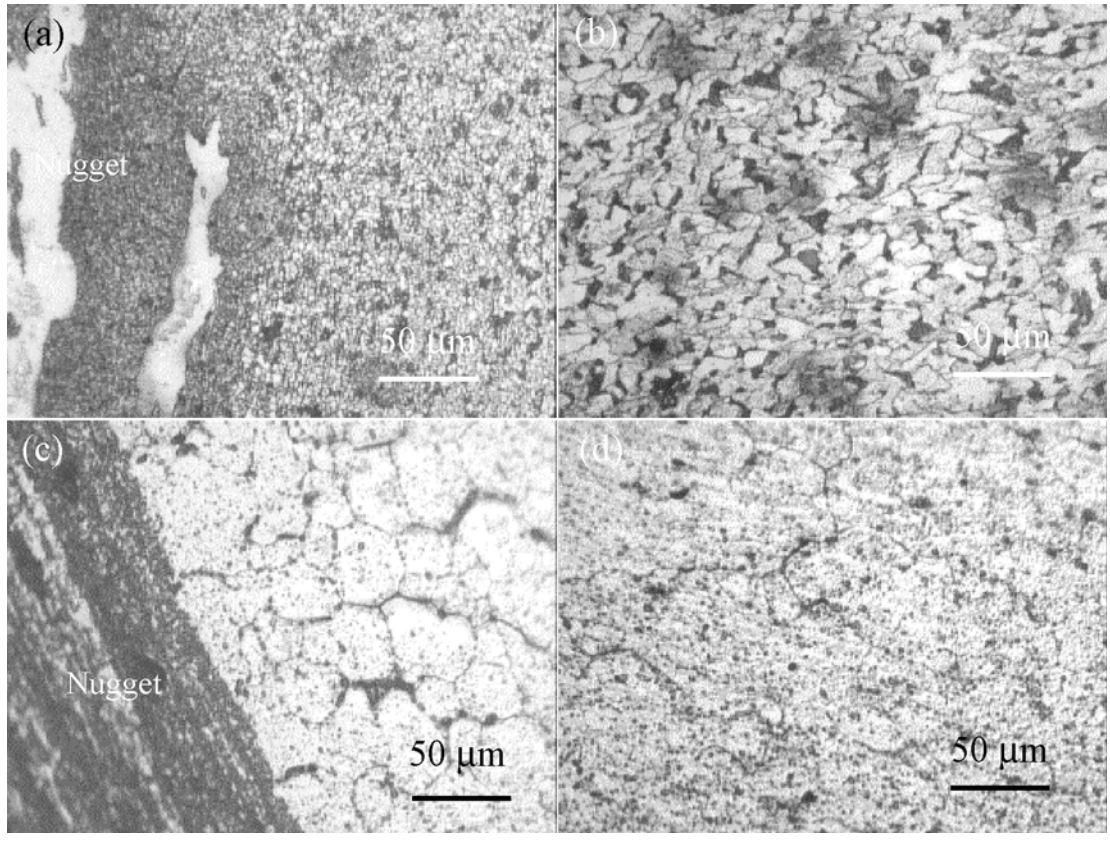

Fig. 13 Microstructures of TMAZs in (a) steel and (c) Al alloy and of (b) the base steel and (d) Al alloy

strain rates, as well as the highest temperature. The formation and evolution of phases in a nugget are rather complex due to the effect of both heat and mechanical force in a very short period of time. The constituent phases in the nugget must be in a thermodynamic non-equilibrium state during processing. Although only the intermetallic compounds of $Al_{13}Fe_4$ and Al_5Fe_2 were detected by X-ray diffraction analysis, there may be some unidentified intermetallic compounds in the nugget whose contents may be too small to be detected.

From the microstructural observations and temperature measurement, it can be deduced that, during FSW, local melting of the Al alloy in the nugget may have occurred. The main evidence is as follows:

1. The temperature measurement demonstrates that the maximum temperatures in the steel and Al alloy adjacent to the nugget are 613 and 491 °C respectively and therefore it is expected that some locations in the nugget have a temperature surpassing the solidus temperature (582 °C).
2. Few intercalated microstructures and vortices can be seen and most steel pieces are disconnected completely from the base steel and distributed within the nugget.
3. Within the nugget, the reaction between the steel pieces and the Al alloy is very aggressive as evidenced by the fact that a significant number of steel pieces are exhausted and the reaction happened even at the boundary between the nugget and the base steel.
4. The fine precipitates are well distributed and not segregated around the reacted steel pieces, despite the fact that their formation is closely related to the evolution of the reaction layer around the steel pieces, which may be attributed to the good fluidity.
5. Many precipitates assume the flower petal shape that is a typical morphology of a phase growing during solidification. It needs to be pointed out that the temperature of the nugget is not high enough to melt steel, which is evidenced by the existence of numerous steel pieces through the nugget (Fig. 6) as well as by the measured temperature, although the high temperature caused dynamic recrystallization of the severely deformed steel pieces, as shown in Fig. 11a.

Following the above discussion, it can be envisaged that FSW results in the formation of a local partial molten Al alloy in the nugget. The steel pieces in the nugget react with the molten Al alloy aggressively under strong mechanical stirring. The reaction layer was formed at the surface of the steel pieces. However, the initially formed Al–Fe phase is unstable and tends to separate from the reaction layer. Some particles of the phase may dissolve into the melt, resulting in an

increase in the content of Fe in the melt. Upon subsequent cooling, an Al–Fe phase may reprecipitate and grow into various morphologies. Undoubtedly, the observed morphologies of the precipitates are related to a local chemical constitution, cooling rate and even mechanical stirring. Indeed, large flower petal phases are observed only among the coarse steel pieces and in the regions adjacent to the base steel. It is believed that in these regions the flow of the Al alloy matrix is small and the local content of Fe is kept high, while in the region bounding the base Al alloy with the nugget, a number of fine sphere-like precipitates exist where the flowing lines of the material are evident (Fig. 9). It is worthy of mention that the reaction of steel pieces with Al melt destroys the overall continuous flow and plastically deformed morphologies of the steel pieces, despite the fact that a few discrete steel pieces display flowing lines themselves. Near the boundary of the nugget with the Al alloy side, no steel pieces are visible and secondary phase particles are very fine.

It is well known that FSW is characterized as a solid-state welding process. During FSW, heating of the workpiece material is caused by rubbing of the tool shoulder against the top surface of the workpiece and by visco-plastic dissipation of the mechanical energy generated by the tool pin. This heating results in a softening of the workpiece material and promotes its plastic flow. It has been found that for friction stir welded Al alloys, a microstructural evolution includes mainly the dissolution of the secondary phases and a continuous dynamic recrystallization [**15**–**18**]. However, no melting is found during FSW of both similar and dissimilar alloys, such as 6061Al/6061Al, 304L stainless steel/304L stainless steel, 6061Al/2024Al and 6061Al/Cu. In the nugget of the friction stir welded Al and copper, the reaction layer was observed in an intercalated Al and Cu laminae that formed through solid-state diffusion aided by mechanical deformation [**10**–**12**]. It is believed that during FSW, the local partial melting of the workpiece material in a nugget could occur only in the case of welding dissimilar alloys with a significant difference in the melting point, such as Al and steel as shown in the present work. Due to its higher melting point, steel has a higher deformation resistance at elevated temperatures. As a significant deformation is indispensable in FSW, higher temperatures must be attained so as to soften and, thus, deform the steel substantially. Higher temperatures can be attained by increasing the rotational speed. Consequently, higher temperatures are developed that surpass the solidus temperature of the Al alloy, resulting in the formation of a localized partial melting zone of the Al alloy in the nugget.

To the authors' best knowledge, the formation of intermetallic compounds in various fusion welds of Al alloy and steel is also unavoidable. A continuous intermetallic layer usually forms at the interface between Al alloy and steel. In order to reduce the deleterious effect of the intermetallic compounds, their layer thickness needs to be minimized through optimizing processing parameters. It has been demonstrated that minimized intermetallic compound layer thickness of less than 10 μm would result in good mechanical properties [**19**]. In the present work, although the nugget of FSW of the Al alloy and steel contains Al–Fe intermetallic compounds, they are small with respect to the volume of Al alloy and steel and well distributed, and their size is rather small. Furthermore, at the boundary zone between the nugget and base steel, the intermetallic compound layer thickness is even less than 5 μm. Therefore, it is believed that it would not worsen the mechanical properties of the weld. This microstructural feature is attributed to strong mechanical stirring, rapid cooling, as well as a relatively low weld temperature. Evidently, it is substantially different from the fusion welding of Al alloys and steels. It is expected that the presence of discrete, well-distributed Al–Fe intermetallic compounds in the nugget may not be detrimental to the mechanical properties of the weld; on the contrary, these compounds could be beneficial. The nugget can be taken as an aluminium matrix composite reinforced by steel and Al–Fe intermetallic compounds. It is worthy to mention that Rathod and Kutsuna recently attributed embrittlement of a weld of Al alloy and steel to the formation of Kirkendall porosity rather than the intermetallic compound layer [**20**]. In the present work, the weld is free of porosity and cracks, and has an excellent quality.

The present work indicates that the microstructure of the nugget is rather complex and that further study needs to be performed in order to identify phases, their evolution and the corresponding mechanisms.

5 CONCLUSIONS

The results of this work could be summarized as follows:

1. FSW is a feasible route to join 6061 Al alloy and AISI 1018 steel, and the weld has a good weld quality and is free of cracks and porosity.
2. The tensile failure occurred at the boundary between the nugget and the thermomechanically affected zone of the base Al alloy, indicating that the weld has a high joining strength.
3. Despite the hardness that fluctuates strongly within the nugget, the average hardness of the nugget is much higher than that of the base Al alloy.
4. During FSW, the Al alloy in the nugget melted locally and reacted strongly with steel pieces, resulting in the formation of the Al–Fe intermetallic compounds, $Al_{13}Fe_4$ and Al_5Fe_2.
5. The nugget consists of secondary phases including coarse steel pieces, coarse and fine Al–Fe intermetallic compounds and an Al alloy matrix. The secondary phases contribute to the hardness of the weld.

ACKNOWLEDGEMENTS

The authors acknowledge the help of Mr M. Valant and Dr C. M. Chen in the execution of the experimental work.

REFERENCES

1 **Sahin, A. Z., Yilbas, B. S.** and **Al-Garni, A. Z.** Friction welding of Al–Al, Al–steel, and steel–steel samples. *J. Mater. Engng Performance*, February 1996, **5**(1), 89–99.

2 **Kawai, G., Ogawa, K., Ochi, H.** and **Tokisue, H.** Friction welding of various aluminum alloy pipe to SUS304 stainless steel pipe. *J. Japan Inst. Light Metals*, February 1999, **49**(2), 83–88.

3 **Kawai, G., Ogawa, K., Ochi, H.** and **Tokisue, H.** Friction weldability of aluminum alloy to carbon steel. *J. Light Metal Weld. Constr.*, July 1999, **37**(7), 295–302.

4 **Fukumoto, S.** Formation process of reaction layer between aluminum alloy and stainless steel by friction welding. *J. Light Metal Weld. Constr.*, 2002, **40**(5), 22–28.

5 **Watanabe, T., Yoneda, A., Yanagisawa, A., Konuma, S.** and **Ohashi, O.** Ultrasonic welding of Al–Cu and Al–SUS304—study on the ultrasonic welding of dissimilar metals (First report). *Q. J. Japan Weld. Soc.*, May 1999, **17**(2), 223–233.

6 **Lienert, T. J., Stellwag Jr, W. L., Grimmett, B. B.** and **Warke, R. W.** Friction stir welding studies on mild steel. *Weld. J. (Suppl.)*, January 2003, **82**, 1s–9s.

7 **Tang, W., Reynolds, A. P., Gnaupel-Herold, T.** and **Prask, H.** Structure, properties, and residual stress of 304L stainless steel friction stir welds. *Scr. Materialia*, May 2003, **48**, 1289–1294.

8 **Watanabe, T., Takawama, H., Kimapong, K.** and **Hotta, N.** Joining of steel to aluminium alloy by interface-activated adhesion welding. *Mater. Sci. Forum*, 2003, **426–432**, 4129–4134.

9 **Chen, C. M.** and **Kovacevic, R.** Joining of Al6061 alloy to AISI 1018 steel by combined effects of fusion and solid state welding. *Int. J. Mach. Tools Mf.*, 2004, **44**(11), 1205–1214.

10 **Murr, L. E., Li, Y., Trillo, E. A., Flores, R. D.** and **McClure, J. C.** Microstructures in friction-stir welded metals. *J. Mater. Processing Mfg Sci.*, 1998, **7**(2), 145–161.

11 **Murr, L. E., Li, Y., Flores, R. D., Trillo, E. A.** and **McClure, J. C.** Intercalation vortices and related microstructural features in the friction-stir welding of dissimilar metals. *Mater. Res. Innovation*, November 1998, **2**(3), 150–163.

12 **Ouyang, J. H.** and **Kovacevic, R.** Materials flow and microstructure in the friction stir butt welds of the same and dissimilar aluminum alloys. *J. Mater. Engng Performance*, January 2002, **11**(1), 51–63.

13 **Liu, H., Fujii, H., Maeda, M.** and **Nogi, K.** Tensile properties and fracture locations of friction-stir welded joints of 6061-T6 aluminum alloy. *J. Mater. Sci. Lett.*, August 2003, **22**(15), 1061–1063.

14 **Sato, Y. S.** and **Kokawa, H.** Distribution of tensile property and microstructure in friction stir weld of 6063 aluminum. *Metall. Mater. Trans.*, 2001, **32A**, 3023–3031.

15 **Murr, L. E., Liu, G.** and **McClure, J. C.** TEM study of precipitation and related microstructures in friction-stir-welded 6061 aluminum. *J. Mater. Sci.*, March 1998, **33**, 1243–1251.

16 **Sato, Y. S., Kokawa, H., Enomoto, M.** and **Jogan, S.** Microstructural evolution of 6063 aluminum during friction-stir welding. *Metall. Mater. Trans.*, September 1999, **30A**, 2429–2437.

17 **Mahoney, M. W., Rhodes, C. G., Flintoff, J. G., Spurling, R. A.** and **Bingel, W.** Properties of friction-stir-welded 7075 T651 aluminum. *Metall. Mater. Trans. A*, July 1998, **29A**, 1955–1964.

18 **Jata, K. V.** and **Semiatin, S. L.** Continuous dynamic recrystallization during friction stir welding of high strength aluminum alloys. *Scr. Materialia*, September 2000, **43**, 743–749.

19 **Sepold, G.** and **Kreimeyer, M.** Joining of dissimilar materials. In Proceedings of the First International Symposium on *High-Power Laser Macroprocessing* (Eds I. Miyamoto, K. F. Kobayashi, K. Sugioka, R. Poprawe and H. Helvajian), Osaka, Japan, 27–31 May 2002; also in *Proc. SPIE*, 2003, **4831**, 526–533.

20 **Rathod, M. J.** and **Kutsuna, M.** Joining of aluminum alloy 5052 and low carbon steel by laser roll welding. *Weld. J. (Suppl.)*, January 2004, **83**, 16s–26s.